Journal of Theoretical and Applied Information Technology
15th March 2026. Vol.104. No.5

ISSN: 1992-8645 www.jatit.org E-ISSN: 1817-3195

IMPROVEMENT OF ANFIS FOR EARLY CARDIOVASCULAR DISEASE PREDICTION MODEL USING DIFFERENTIAL EVOLUTION (DE) AND LIME EXPLAINABLE AI

SRI SUMARLINDA[1], WIJI LESTARI[2], FAULINDA ELY NASTITI[3]

[1,2,3]Faculty of Computer Science, University of Duta Bangsa Surakarta, Indonesia

E-mail: [1]sri_sumarlinda@udb.ac.id, [2]wiji_lestari@udb.ac.id, [3]faulinda_ely@udb.ac.id

ABSTRACT

The early detection of cardiovascular disease (CVD) remains a critical challenge in preventive healthcare, requiring predictive models that are both accurate and interpretable. This study aims to develop an early CVD prediction model enhanced with Differential Evolution (DE) optimisation and explainable AI using LIME. The models were evaluated on a dataset of 500 samples comprising six features: age, body mass index (BMI), systolic blood pressure, diastolic blood pressure, cholesterol, and blood sugar. The ANFIS model was improved by optimising its premise and consequent parameters through mutation, crossover, and selection processes within the DE algorithm. LIME was employed to provide interpretability by revealing the contribution of each feature to the ANFIS-DE prediction outcomes. The dataset was evaluated using three different data-splitting schemes to identify the most effective training testing proportion. In Model 1, the data were divided into 60% for training and 40% for testing. Model 2 applied a 70%:30% split, whereas Model 3 used an 80%:20% split. Among these configurations, Model 3 (80%:20%) yielded the highest predictive performance, indicating that a larger portion of training data contributed to better model generalisation and overall accuracy. The enhanced ANFIS-DE model outperformed the baseline ANFIS, achieving higher testing accuracy (0.9200 vs. 0.9167), precision (0.9290 vs. 0.9287), recall (0.9250 vs. 0.9250), and F1-score (0.9425 vs. 0.9367), alongside a lower error value (0.2011 vs. 0.2019). LIME analysis further indicated that blood sugar had the highest contribution (0.27), followed by systolic blood pressure (0.25), age (0.20), cholesterol (0.06), BMI (0.03), while diastolic blood pressure exerted a slight negative influence (–0.01), demonstrating the usefulness of feature-level explanations in supporting early CVD risk prediction.

Keywords: *Cardiovascular Disease, ANFIS, Differential Evolution (DE), LIME Explainable AI, Early Prediction Model*

1. INTRODUCTION

Cardiovascular disease (CVD) remains the leading cause of death worldwide, accounting for approximately 32% of global mortality according to the World Health Organization (WHO, 2023). Each year, more than 17.9 million people die from CVD, which includes conditions such as coronary artery disease, stroke, and heart failure, many of which are preventable through early diagnosis, effective clinical management, and lifestyle modification[1]. Despite this, early detection and prevention of CVD remain major global health challenges, particularly in developing countries where limited healthcare resources, fragmented health information systems, and low public awareness hinder effective disease control [2].

The Adaptive Neuro-Fuzzy Inference System (ANFIS) and Differential Evolution (DE) are two widely used computational approaches in the development of modern predictive and optimization models due to their complementary strengths. ANFIS combines the flexibility of fuzzy logic with the learning capability of neural networks to construct nonlinear relationships that can be interpreted through fuzzy rules, making it suitable for applications requiring transparency in decision-making. However, ANFIS has limitations in capturing temporal dynamics and complex sequential patterns [3], [4]. [5], [6]. Conventional ANFIS training procedures, which employ gradient descent in conjunction with least-squares estimation, are frequently characterized by sluggish convergence, a pronounced susceptibility to entrapment in local minima, diminished

optimization capability when addressing complex modelling tasks, and a marked sensitivity to initial parameter configurations [4]. [5], [6].

Differential Evolution (DE) has emerged as a highly effective evolutionary optimization technique, particularly valued for its ability to navigate complex, multi-dimensional search spaces commonly encountered in medical data analysis. Unlike traditional gradient-based methods, DE performs global optimization through population-based mutation and recombination, enabling it to avoid premature convergence and local minima. This characteristic is particularly important in medical prediction tasks, where the data are often noisy, nonlinear, and imbalanced. The robustness, stable convergence behavior, and minimal reliance on initial parameter settings make it exceptionally suitable for refining model parameters, enhancing predictive accuracy, and improving the reliability of computational models in clinical decision-support scenarios [7], [8], [9], [10], [11]

Several studies have been conducted to improve the performance of ANFIS as a predictive model. One commonly used approach is the application of clustering techniques in data mining to determine the membership functions in the input layer. In addition, ANFIS has been further developed through integration with Genetic Algorithms (GA) to form hybrid models capable of enhancing prediction accuracy and efficiency [12],[13],[14]. Other performance enhancement efforts include optimizing model parameters using Particle Swarm Optimization (PSO)[15], [16], [17]. Furthermore, the Grey Wolf Optimizer (GWO) has also been applied as an alternative optimization method and has proven effective in improving the performance of ANFIS in various predictive studies [18], [19], [20], [21].

Improving the performance of predictive models has become increasingly important, particularly in the medical domain, where high accuracy and transparency are essential. Most machine learning and deep learning models operate as black boxes, making it difficult to observe the contribution of individual features in the prediction process. Although ANFIS includes a rule-generation mechanism and is therefore not entirely a black-box model, the contribution of each feature is still not fully transparent. To address this issue, Explainable AI (XAI) can be employed to reveal the role of each feature in generating predictions, both in machine learning models and ANFIS [22], [23], [24]. In general, XAI consists of two primary methods: Local Interpretable Model-Agnostic Explanations (LIME) and SHAP (Shapley Additive Explanations), both of which provide clearer and more quantifiable interpretations of predictive models [25], [26], [27].

In this study, a predictive model based on ANFIS was developed by modifying using Differential Evolution (DE) architecture. The ANFIS prediction model optimized using Differential Evolution (DE) operates through a layered computational pipeline in which fuzzy rules, membership parameters, and consequent parameters are integrated within a unified adaptive neuro-fuzzy framework. The Differential Evolution (DE) is recognized as a powerful evolutionary optimisation method for improving the learning performance of Adaptive Neuro Fuzzy Inference Systems (ANFIS) in early cardiovascular disease prediction. Conventional ANFIS relies on gradient based updates, which are often sensitive to initialisation and prone to convergence toward local minima, especially when processing nonlinear and high dimensional clinical data. DE introduces a global search strategy that systematically refines both the premise parameters in the fuzzy membership functions and the consequent parameters in the Sugeno rules, enabling ANFIS to achieve more accurate and stable inference. Through iterative processes of mutation, crossover, and selection, DE explores diverse candidate solutions and converges toward an optimal configuration of the ANFIS structure. In cardiovascular risk assessment, where complex interactions among variables such as age, blood pressure, cholesterol level, body mass index, and blood sugar strongly affect predictive outcomes, the integration of DE significantly enhances the model's generalisation ability, sensitivity, and reliability, thus supporting more effective early disease detection. Input fuzzification via membership functions, computation of firing strengths, and normalization of rule weights. The principal innovation arises in Layer 4, where the defuzzification of the consequent no longer relies on least-squares estimated parameters, as in conventional ANFIS, but instead employs Differential Evolution to optimize the consequent parameters, enabling each fuzzy rule to generate the most suitable linear or non-linear output for the training data.

Following the generation of predictions, the workflow proceeds with the application of the Explainable AI method LIME, which provides local interpretability for the model's decisions. LIME produces a set of perturbed samples around the input instance and subsequently constructs an interpretable surrogate model, typically a local linear regression, to estimate the contribution of each feature to the final ANFIS-DE output. This process yields a

feature-attribution map indicating the relative influence of age, BMI, systolic blood pressure, diastolic blood pressure, cholesterol, and blood sugar on the predicted cardiovascular risk for each individual patient. The integration of DE and LIME therefore not only enhances predictive accuracy through optimization premise and consequent parameters, but also improves transparency and interpretability, making the approach particularly well suited to medical prediction tasks that demand both high performance and explainable model behaviors.

2. MATERIAL AND METHODS

2.1 DATASET

The dataset consists of clinical data with the features blood sugar, cholesterol, systolic, diastolic, BMI, and age, comprising a total of 500 records. After processing data, the dataset was reduced to 300 records. The dataset was obtained from PKU Surakarta Hospital and comprises samples from both cardiovascular and non-cardiovascular patients.

The use of age, body mass index (BMI), systolic blood pressure, diastolic blood pressure, cholesterol level, and blood sugar concentration as predictive features for early cardiovascular risk assessment is supported by extensive clinical and biomedical evidence, and has been further validated through consultation with medical practitioners and academic experts in cardiovascular health. These variables capture key physiological pathways—such as atherosclerotic progression, metabolic dysregulation, and hemodynamic stress—that are known to precede clinically manifest cardiovascular disease. Medical professionals affirm that these routinely measurable indicators provide a reliable basis for identifying individuals at elevated risk, while academic experts highlight their consistent associations with cardiovascular outcomes across epidemiological and cohort studies. Consequently, the integration of these six features into predictive modelling frameworks is scientifically justified and clinically relevant for early detection strategies.

Moreover, the acquisition of these six features is simple and highly accessible, as modern digital devices including automated blood pressure monitors, portable cholesterol analyzers, and digital blood glucose meters enable fast, user friendly, and reliable data collection both in clinical settings and at home. Medical professionals affirm that these routinely measurable indicators provide a robust basis for identifying individuals at elevated cardiovascular risk, while academic experts highlight their consistent associations with cardiovascular outcomes across epidemiological and cohort studies. Consequently, the integration of these features into predictive modelling frameworks is scientifically justified, clinically relevant, and operationally feasible for early detection strategies.

A sample of the dataset used is presented in Table 1:

Table 1: Sample of Dataset

ID	BLOOD SUGAR	CHOLESTEROL	SISTOLIC	DIASTOLIC	BMI	AGE	OUTPUT
478	120	180	120	90	16	19	0
370	200	150	130	90	16	22	0
100	140	150	120	80	17	19	0
319	140	150	120	80	17	19	0
409	90	112	96	90	17	19	0
106	120	135	105	90	17	18	0
325	120	135	105	90	17	18	0
462	65	180	110	90	17	19	0
121	84	207	108	91	17	20	0
340	84	207	108	91	17	20	0
421	90	122	80	100	17	28	0
391	150	150	100	100	17	20	0
375	117	189	117	60	18	20	0

2.2 ANFIS MODEL ARCHITECTURE

The Adaptive Neuro-Fuzzy Inference System (ANFIS) model integrates the learning capability of artificial neural networks with the reasoning mechanism of fuzzy logic.

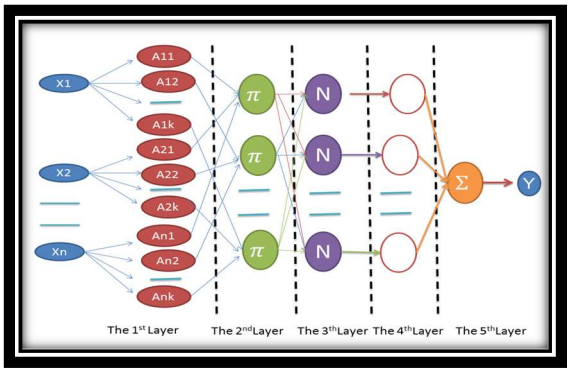

Figure 1. ANFIS Model Architecture

The ANFIS model has 5 layers, 1st layer is data input processing, we use Gaussian memberships function with formula:

$$\mu(x) = \frac{1}{1+\left|\frac{x-c}{a}\right|^{2b}} \quad (1)$$

where: μ(x) is membership function, a, b, c are premise parameters.

The 2nd layer is the multiplication of the membership degrees. The formula in 2nd layer:

$$w_k = \prod_1^n \mu_{nk} = \mu_{1k}.\mu_{2k}.\mu_{3k} \dots \mu_{nk} \quad (2)$$

where: w_k is multiplication of the membership degrees

The 3rd layer is the weight-to-weight ratio calculation, with formula:

$$\bar{w}_k = \frac{w_k}{\sum_1^k w_k} = \frac{w_k}{w_1+w_2+w_3+\cdots+w_k} \quad (3)$$

The 4th layer is processing that each neuron in the fourth layer is an adaptive node to an output:

$$\bar{w}_k . y_k = \bar{w}_k (c_{k1} . x_1 + c_{k2} . x_2 + c_{k3} . x_3 + \cdots + c_{kn} . x_n + c_{k0} \quad (4)$$

The 5th layer is processing output with formula:

$$y = \sum_1^k \bar{w}_k . y_k = \bar{w}_1 . y_1 + \bar{w}_2 . y_2 + \bar{w}_3 . y_3 + \cdots + \bar{w}_k . y_k \quad (5)$$

2.3 DIFFERENTIAL EVOLUTION (DE)

The Differential Evolution (DE) is a stochastic population based on optimization algorithm widely recognized for its effectiveness in solving high dimensional and multimodal optimization problems with strong computational efficiency. Operating without derivatives, DE is well suited for objective functions that are noisy, discontinuous, or analytically difficult to model, where gradient based methods often fail. Its optimization process relies on three key operators, mutation, crossover and selection, which collectively refine candidate solutions through adaptive exploration and convergence [7], [11], [28], [29]. In particular, the mutation step perturbs a base vector using the scaled difference of two population vectors, enabling broad search space exploration and reducing the risk of premature convergence to local optima. Owing to its robust convergence behavior and consistent empirical performance, DE has become a prominent choice in advanced optimization tasks across machine learning, biomedical modelling and complex system identification. The are 3 steps in DE, namely mutation, crossover and selection[10], [11], [28].

The formula of mutation:

$$\boldsymbol{v_i} = \boldsymbol{x_p} + \boldsymbol{\mu} . (\boldsymbol{x_q} - \boldsymbol{x_r}) \quad (6)$$

Where:

$\boldsymbol{v_i}$ is mutated vector

$\boldsymbol{x_p}$, $\boldsymbol{x_q}$, $\boldsymbol{x_r}$ are distinct vectors randomly chosen from the current population

$\boldsymbol{\mu}$ is the mutation scaling factor

The formula of crossover:

$$u_{i,j} = \begin{cases} v_{i,j}, & if\ Rand_j \le C_R\ or\ j = j_{rand} \\ x_{i,j,} & otherwise \end{cases} \quad (7)$$

Where:

$\boldsymbol{u_{i,j}}$ is the j^{th} component of the trial vector for the i^{th} individual.

$\boldsymbol{v_{i,j}}$ is the j^{th} component of the mutated vector.

$\boldsymbol{x_{i,j}}$ is the j^{th} component of the target vector.

C_R is crossover rate

j_{rand} is a randomly chosen index to ensure that at least one component of the trial vector comes from the mutated vector.

The selection process is given by:

$$x_i^{t+1} = \begin{cases} u_i^{t+1}, & if\ f(u_i^{t+1}) \le f(x_i^t) \\ x_i^t & otherwise \end{cases} \quad (8)$$

x_i^{t+1} is represents the updated solution for the i^{th} individual in the next generation.

u_i^{t+1} is trial vector

f(.) is objective function

2.5 LIME XAI

Explainable AI using Local Interpretable Model Agnostic Explanations (LIME) provides a systematic framework for understanding how complex machine learning models make individual predictions. LIME operates by generating a set of perturbed samples around a specific instance and evaluating how the model responds to these variations. It then constructs a simple, interpretable surrogate model, typically a local linear regression, to approximate the behaviour of the original model in the neighbourhood of that instance. Through this process, LIME quantifies the contribution of each feature to the predicted outcome, enabling researchers and practitioners to obtain intuitive and human readable explanations without requiring access to the internal structure of the model [30], [31].

The formula of LIME XAI:

$$\arg\min_{g \epsilon G} L(f, g, \pi_x) + \Omega(g) \quad (9)$$

Where:

g is the interpretable model used to approximate the complex model locally.

G is the family of interpretable models from which g is selected.

$L(f, g, \pi_x)$ is the local fidelity loss, which measures how closely the interpretable model g matches the predictions of the original model f around the instance x.

$\Omega(g)$ is a complexity penalty that ensures the surrogate model remains simple and easy to interpret.

2.6 PROPOSED MODEL

The proposed model integrates ANFIS with Differential Evolution to optimise parameter learning and enhance predictive accuracy, while XAI LIME is employed to provide transparent, instance-level explanations of the model's outputs. Six input features are processed through the ANFIS structure, refined through iterative mutation mechanism of DE, and subsequently interpreted using LIME to ensure both robust performance and explainability. The model shown in figure 2.

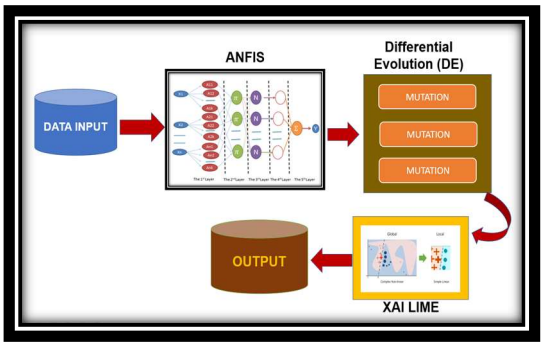

Figure 2. Model Optimation Architecture

The predictive workflow proceeds in six clear steps. Step 1: normalise the six clinical features blood sugar, cholesterol, systolic pressure, diastolic pressure, BMI and age. Step 2: construct an ANFIS architecture with Gaussian membership functions, where each function is parameterised by a mean and a spread and each fuzzy rule uses a Takagi Sugeno first order consequent. Step 3: encode every premise parameter and every consequent coefficient into a single optimisation vector. Step 4: refine that vector with Differential Evolution, employing mutation, crossover and selection to minimise a validation error objective and thus reduce susceptibility to the local optima that impede conventional gradient based ANFIS training. Step 5: evaluate the optimised ANFIS on a held out test set to produce final performance metrics. Step 6: generate local explanations with LIME by creating perturbed samples around the instance, querying the trained ANFIS, weighting samples by proximity and fitting a sparse linear surrogate to reveal the relative contribution of each feature to the specific prediction.

To enhance predictive accuracy and ensure stable convergence, the ANFIS parameters are optimised using the Differential Evolution (DE) algorithm. DE operates as a population-based evolutionary optimiser that iteratively refines candidate solutions through mutation, crossover, and fitness-based selection. At each generation, the algorithm applies controlled perturbations to the parameter vectors, recombines them to produce trial solutions, and retains only those that minimise the prediction error. This optimisation process yields an ANFIS model with improved parameter configurations and enhanced generalisation capability.

Following optimisation, the ANFIS-DE model is employed to generate predictions for the target variable. To ensure transparency and support interpretability, particularly in a clinical context, the predictions are further analysed using the Local Interpretable Model-Agnostic Explanations (LIME) framework. LIME constructs perturbed samples around a specific instance and evaluates the corresponding outputs of the ANFIS-DE model. By fitting a local interpretable surrogate model, typically a sparse linear approximation, LIME quantifies the relative contribution of each input feature to the final prediction. This provides a clear and local explanation that complements the optimised model output.

2.7 EVALUATION MODEL

The predictive performance of the proposed model for cardiovascular disease was evaluated using the Adaptive Neuro-Fuzzy Inference System (ANFIS) integrated with Differential Evolution (DE) and Explainable Artificial Intelligence (XAI) through Local Interpretable Model-Agnostic Explanations (LIME). Model evaluation was conducted using a confusion matrix, which provides a comprehensive assessment of classification outcomes. The performance metrics include Accuracy, Recall, Precision, and F1-Score, which are standard measures in prediction model.

Accuracy is defined as the proportion of correctly classified instances to the total number of instances, expressed as:

$$Accuracy = \frac{TP+T}{TP+TN+FP+FN} \quad (10)$$

Precision evaluates the proportion of true positive predictions among all positive predictions, defined as:

$$Precesion = \frac{TP}{TP+FP} \quad (11)$$

Recall (or Sensitivity) measures the model's ability to correctly identify positive cases, given by:

$$Recall = \frac{TP}{TP+FN} \quad (12)$$

Meanwhile, the F1-Score, representing the harmonic mean of Precision and Recall, is calculated as:

$$F1 - Score = 2\,x\,\frac{Precision\ x\ Recall}{Precision+R} \quad (13)$$

where TP, TN, FP, and FN denote true positives, true negatives, false positives, and false negatives respectively.

3. RESULT AND DISCUSSION

3.1 THE ANFIS MODEL PERFORMANCE OVERVIEW

The ANFIS model was trained using a dataset comprising 300 instances with six clinical features, namely blood sugar, systolic blood pressure, diastolic blood pressure, cholesterol, BMI, and age, and a binary output indicating cardiovascular risk 0 (lower susceptibility) or 1 (higher susceptibility).

The Adaptive Neuro-Fuzzy Inference System (ANFIS) was employed to develop an early prediction model for cardiovascular disease. The model was experienced to 3 models. The model 1 (60% training, 40% testing), model 2 (70% training, 30% testing), and model 3 (80% training, 20% testing). Each model was subsequently evaluated using five training epochs (200, 400, 600, 800, and 1000) with learning rate of 0.1. The predictive performance across all models' variations were then compared, with the comparative results presented in Table 2 and illustrated in Figure 3.

Table 2: Performance of ANFIS Models for CVD prediction

Confusion Metric	Model 1 60%		Model 2 70%		Model 3 80%	
	Training Data	Testing Data	Training Data	Testing Data	Training Data	Testing Data
Accuracy	0.9389	0.9088	0.9398	0.9167	0.9417	0.9167
Precision	0.9431	0.9061	0.9536	0.925	0.962	0.9487
Recall	0.936	0.8875	0.9464	0.9073	0.95	0.925
F1 Score	0.9347	0.9067	0.946	0.9261	0.956	0.9367

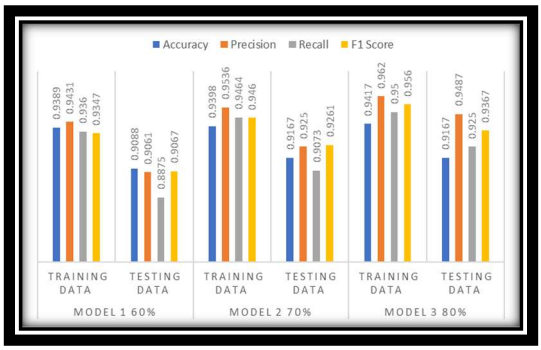

Figure 3. Comparative performance of ANFIS models

Based on Table 2 and Figure 3, Model 3 demonstrates the best predictive performance. Therefore, Model 3 was selected for performance improvement using the Differential Evolution (DE) algorithm. The results of the optimisation processes applied to Model 3 are presented in Figure 4.

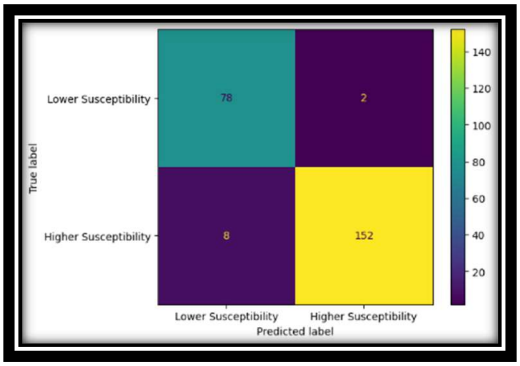

Figure 4. Predicted table

The confusion matrix illustrates in figure 4, the classification performance of the model in distinguishing between lower susceptibility and higher susceptibility classes. The model correctly identified 78 instances of lower susceptibility and 152 instances of higher susceptibility, indicating strong predictive capability for both classes. Only 2 cases of lower susceptibility were incorrectly classified as higher susceptibility, while 8 cases of higher susceptibility were misclassified as lower susceptibility. Overall, the distribution of correct and incorrect predictions demonstrates that the model achieves high accuracy and maintains balanced performance across both categories, with notably low misclassification rates.

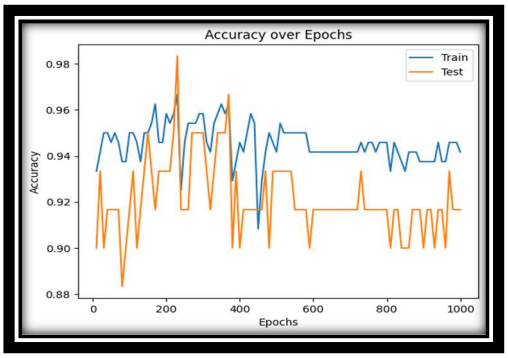

Figure 5. Accuracy of Model ANFIS

According to figure 5, the plot presents the progression of training and testing accuracy over 1000 epochs. The training accuracy curve shows a generally stable upward trend during the early epochs, reaching values consistently above 0.94 after convergence. Minor fluctuations occur, but the

overall pattern indicates that the model learns effectively and maintains high performance on the training data. The testing accuracy curve, although more variable, remains within a high accuracy range throughout training, typically oscillating between 0.90 and 0.96. This variability suggests sensitivity to the smaller test sample but still reflects strong generalization capability. The absence of significant divergence between the two curves indicates that the model does not experience severe overfitting, and both training and test performances remain consistently high across epochs.

3.2 IMPROVEMENT ANFIS MODEL USING DIFFERENTIAL EVOLUTION(DE)

The optimisation of the Adaptive Neuro-Fuzzy Inference System (ANFIS) using Differential Evolution (DE) is conducted to obtain an optimal set of premise and consequent parameters for binary cardiovascular risk prediction based on six clinical features: Blood Sugar, Systolic Blood Pressure, Diastolic Blood Pressure, Cholesterol, BMI, and Age. In the initial configuration, each membership function is defined by premise parameters typically denoted as *a*, *b*, and *c*-while each fuzzy rule is associated with a set of consequent parameters, such as $k_{11}, k_{21}, \ldots, k_{61}$, representing the linear coefficients for the input variables.

The DE algorithm begins by generating a population of candidate solutions, where each individual encodes a complete parameter set of the ANFIS model, including all premise and consequent components. Each individual is evaluated through forward computation within ANFIS, and its fitness is calculated using a binary classification metric such as cross-entropy loss or misclassification rate.

The optimisation proceeds iteratively through three fundamental evolutionary operators. First, **mutation** perturbs individuals by combining randomly selected population members according to

$$\boldsymbol{v_i} = \boldsymbol{x_a} + \boldsymbol{\mu}.(\boldsymbol{x_b} - \boldsymbol{x_c}) \quad (14)$$

where μ is a scaling factor and v_i is the mutant vector. Second, **crossover** recombines the mutant vector with the original individual to produce a trial vector, governed by a crossover rate that determines the proportion of inherited parameters. Third, **selection** ensures survival of the fittest by replacing the current individual with the trial vector only if the latter exhibits superior fitness.

This cycle continues until convergence or a maximum number of generations is reached. The final solution represents the optimised set of membership-function parameters a, b, c and consequent coefficients k that collectively minimise prediction error. When integrated into ANFIS, these optimised parameters enhance the model's ability to discriminate between classes 0 and 1, thereby improving its predictive accuracy for cardiovascular risk assessment.

Table 3: Comparative performance of ANFIS and ANFIS-DE models Using Confusion Matrix

Confusion Matrix & Error/loss	ANFIS		ANFIS-DE	
	Data Training	Data Testing	Data Training	Data Testing
Accuracy	0.9417	0.9167	0.9458	0.9200
Precision	0.9620	0.9287	0.9656	0.9290
Recall	0.9500	0.9250	0.9625	0.9250
F1 Score	0.9560	0.9367	0.9595	0.9425
Error	0.1685	0.2019	0.1501	0.2011

Based on Table 3, Differential Evolution demonstrably improves the performance of ANFIS. All confusion matrix values for ANFIS DE are superior to those of the standard ANFIS model. Likewise, the error metrics obtained from ANFIS DE are consistently lower than those produced by ANFIS alone.

3.3 FEATURE IMPORTANCE AND EXPLAINABILITY ANALYSIS USING LIME

The Local Interpretable Model-Agnostic Explanations (LIME) method was applied to ANFIS-DE model to improve performance. LIME provided local feature-level explanations for individual predictions by approximating the complex model behavior with an interpretable surrogate model. Figure 3 illustrates an example LIME explanation for a positive (CVD) prediction generated by the ANFIS-DE model. The outcomes of the LIME XAI analysis further provide a visual representation of the contribution of each feature, as illustrated in the following figure 6 bellow.

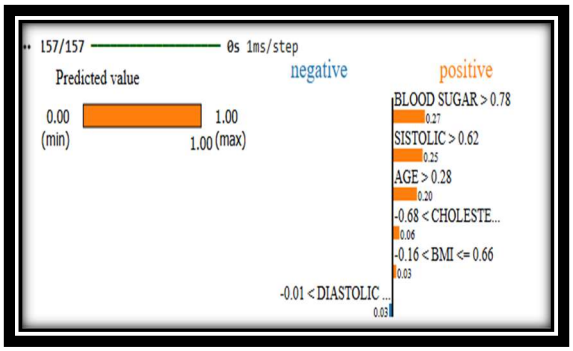

Figure 6. The Features Mapping Using XAI LIME

Conversely, features such as exercise-induced angina and fasting blood sugar were found to contribute negatively to the disease risk prediction for this instance.

When applied to the ANFIS model, LIME explanations closely aligned with the fuzzy rule base, validating the consistency between rule-based inference and local model approximations. For example, ANFIS generated interpretable rules such as:

IF (cholesterol is high) AND (blood pressure is high) THEN (risk = high).

This rule corresponded directly with the high-weight features identified by LIME, demonstrating that both models captured similar clinical risk patterns, though through different representational mechanisms.

Explainable Artificial Intelligence (XAI) using Local Interpretable Model-Agnostic Explanations (LIME) was employed to provide a deeper understanding of the contribution of individual predictive features within the model. The outcomes of the explainable model using LIME analysis are presented in the following table 4.

Table 4. Result of LIME Processing

No	Feature	Contribution	Value
1	Blood Sugar	0.27	1.35
2	Sistolic	0.25	0.84
3	Age	0.20	0.31
4	Cholesterol	0.06	0.12
5	BMI	0.03	0.43
6	Diastolic	-0.01	0.19

The figure 6 and table 4 illustrates the local explanation generated by LIME for a single test instance (one patient). The model outputs a predicted value close to 1, indicating a high estimated cardiovascular risk. LIME decomposes this prediction into feature-level contributions, showing which inputs increase or decrease the model's output. On the right-hand side, the horizontal bars represent the magnitude and direction of each feature's influence. Orange bars correspond to positive contributions, meaning these features push the prediction toward a higher risk. Blue bars indicate negative contributions, where the feature slightly reduces the predicted risk.

The most influential positive contributors for this instance are:

1. BLOOD SUGAR > 0.78 (value = 1.35):

This feature shows the strongest positive effect, substantially elevating the predicted risk.

2. SISTOLIC > 0.62 (value = 0.84):

A high systolic blood pressure further increases the prediction.

3. AGE > 0.28 (value = 0.31):

Although moderate, age still contributes positively to the risk assessment.

CHOLESTEROL and BMI exhibit smaller positive effects, indicating mild contributions to increasing the model's output. In contrast, diastolic blood pressure (value = 0.19) exerts a minor negative contribution, slightly pulling the prediction downward, though its influence is negligible compared with the dominant risk-elevating features.

Of the six features, blood sugar contributes 0.27, systolic blood pressure contributes 0.25, age contributes 0.20, cholesterol contributes 0.06, BMI contributes 0.03, and diastolic blood pressure contributes –0.01.

The feature-value table at the bottom of the figure displays the original input values for the explained instance, with colours matching their directional influence (orange for positive, blue for negative). Overall, the LIME explanation highlights that blood sugar, systolic pressure, and age are the primary drivers of the model's high-risk prediction for this individual. This demonstrates LIME's ability to produce transparent, instance-specific interpretations for an otherwise opaque neural-network model.

3.4 DISCUSSION

The ANFIS-based cardiovascular disease prediction model has demonstrated satisfactory performance, as reflected in its accuracy exceeding 90%. Nevertheless, the standard ANFIS architecture, which employs the gradient descent method for error propagation and least squares estimation, still exhibits several limitations. These limitations include slow convergence, a tendency to become trapped in local minima, sub-optimal performance when addressing complex problems, and high sensitivity to initial parameter values [32], [33], [34].

In this study, the performance of ANFIS was enhanced through integration with the Differential Evolution (DE) algorithm. The hybrid model, referred to as ANFIS-DE, was designed to optimise both the fuzzy premise parameters and consequent parameters within the ANFIS structure.

DE begins by generating a population of ANFIS candidate models with randomly initialised parameters. The mutation process in DE is

performed by computing the differences between candidate solutions to produce new and potentially more diverse candidates. This is followed by a crossover operation to further increase solution diversity within the population.

The selection stage in DE is based on the ANFIS error value, where the candidate with the best performance is retained for the next generation. Through iterative evolutionary processes over multiple generations, DE is able to identify a more optimal combination of ANFIS parameters. The best parameters obtained are subsequently applied to the prediction model to generate improved output accuracy.

The comparative results between the standard ANFIS model and the ANFIS-DE model are presented in Figure 7

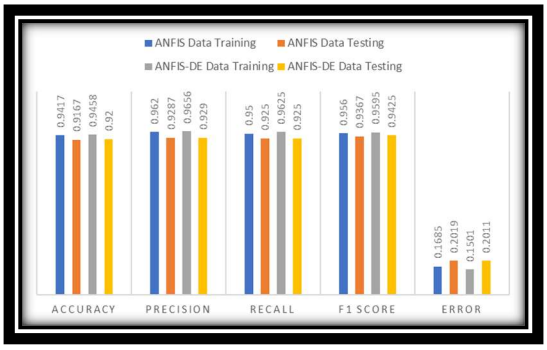

Figure 7. Improvement performs using DE

Based on Figure 7, the confusion matrix results indicate that the ANFIS-DE model achieves higher values of accuracy, precision, recall and F1-score compared with the standard ANFIS model. In addition, the error produced by ANFIS-DE is lower than that of ANFIS. These findings demonstrate that the ANFIS-DE model successfully enhances the predictive performance of the original ANFIS model.

This performance improvement can be attributed to several factors. First, the population-based global evolutionary mechanism of DE enables a more effective optimisation process. Second, the use of DE helps reduce the risk of the model becoming trapped in local minima. Third, DE enhances the exploration capability of the search space, allowing the model to identify more optimal solutions. Fourth, DE facilitates more efficient parameter tuning within the ANFIS structure, resulting in a better overall parameter configuration [29], [35].

The integration of Differential Evolution (DE) into the ANFIS model led to a statistically significant enhancement in performance. Specifically, the accuracy improved from 0.9417 for the standalone ANFIS model to 0.9458 for the ANFIS-DE model. In addition, the error rate was reduced from 0.1685 to 0.1501, indicating superior predictive performance.

The performance of ANFIS can also be enhanced using various alternative methods. Based on existing studies, multiple approaches for improving ANFIS performance can be compared with the proposed model in this research. This comparison is presented in the following table 5

Table 5 Comparison of ANFIS Model Improvement

IMPROVMENT OF ANFIS MODELS	ERROR	ACCURACY	F1-SCORE
K-Medoids Clustering	-	82.99%	-
Genetic Algorithm	0.8977	90.35%	-
PSOGA (ANFIS-PSOGA)	-	91.83%	-
ANFIS-PSO Experiment (UCI Global Data)	-	89.00%	89.00%
ANFIS-PSO	0.282	-	-
PSO-ANFIS	0.928	-	-
GA-ANFIS	0.8977	-	-
ANFIS-DE	0.2011	92%	94.25%

Based on Table 5, it can be observed that the ANFIS-DE model has achieved superior predictive performance.

In general, prediction models developed using machine learning or artificial intelligence operate as black-box systems, meaning that the internal decision-making process does not explicitly reveal which features contribute most to the prediction. Explainable AI techniques, such as LIME, help illustrate the contribution of individual features to the model's output. Through this approach, it becomes clear which features drive the prediction upward and which features contribute to reducing the predicted value [30], [31]

The results of the XAI-LIME analysis for the ANFIS-DE model are presented in Figure 6. The most influential positive contributors in this instance are Blood Sugar (value = 1.35), Systolic Blood Pressure (0.84), and Age (0.31), all of which strongly drive the prediction towards a higher risk. Cholesterol and BMI provide smaller positive effects. Conversely, Diastolic Blood Pressure (0.19) exhibits a minor negative influence, though its effect is negligible compared with the dominant risk-elevating features.

The blood sugar feature plays the most significant role in this prediction model, followed by systolic blood pressure and age. Among the six features used in the prediction model, five features have positive contributions, with blood sugar having the greatest

influence, followed by systolic blood pressure. Only one feature, diastolic blood pressure, shows a negative contribution. Given that systolic and diastolic blood pressure are both indicators of cardiovascular pressure, it can be inferred that blood pressure–related features collectively exert a positive influence on the prediction model.

4. CONCLUTION

The development of an early cardiovascular disease prediction model using ANFIS enhanced with Differential Evolution (DE) and LIME XAI demonstrates a substantial improvement in predictive performance. The original ANFIS model suffers from several limitations, including difficulties in converging reliably and a tendency to become trapped in local optima. These weaknesses are effectively addressed through the application of DE, which optimises the premise and consequent parameters via mutation, crossover, and selection mechanisms. As a result, the ANFIS-DE model achieves higher accuracy, precision, recall, and F1-score across both the training and testing datasets, while also producing a lower error rate compared with the standard ANFIS model.

The integration of LIME XAI enhances model transparency by identifying the relative contribution of each input feature to the ANFIS-DE predictions. The LIME analysis shows that blood sugar, systolic blood pressure, and age are the most influential features, with five of the six features contributing positively and only diastolic blood pressure exhibiting a slight negative effect. Overall, the interpretability provided by LIME XAI confirms that all features play a meaningful role in shaping the predictive performance of the ANFIS-DE model, reinforcing its suitability for early detection of cardiovascular risk.

5. ACKNOWLEDGMENT

The authors would like to express their sincere gratitude to the Ministry of Education, Culture, Research, and Technology of the Republic of Indonesia (Kemdikbudristek) for the research grant and support provided through the Directorate General of Higher Education (DIKTI), Granted Number 127/C3/DT.05.00/PL/2025

REFERENCES:

[1] F. Mai, R. Del Pinto, and C. Ferri, “COVID-19 and cardiovascular diseases,” *J Cardiol*, vol. 76, no. 5, pp. 453–458, 2020, doi: 10.1016/j.jjcc.2020.07.013.

[2] S. Adabag, P. Zimmerman, D. Lexcen, and A. Cheng, “Predictors of Sudden Cardiac Arrest Among Patients With Post-Myocardial Infarction Ejection Fraction Greater Than 35%,” *J Am Heart Assoc*, vol. 10, no. 14, 2021, doi: 10.1161/jaha.121.020993.

[3] J. Feng, Q. Wang, and N. Li, “An intelligent system for heart disease prediction using adaptive neuro-fuzzy inference systems and genetic algorithm,” *J Phys Conf Ser*, vol. 2010, no. 1, 2021, doi: 10.1088/1742-6596/2010/1/012172.

[4] A. Asemi, A. Asemi, and A. Ko, “Adaptive neuro-fuzzy inference system for customizing investment type based on the potential investors’ demographics and feedback,” *J Big Data*, vol. 10, no. 1, Dec. 2023, doi: 10.1186/s40537-023-00784-7.

[5] D. Duranoğlu, E. Sinan Altın, and İ. Küçük, “Optimization of adaptive neuro–fuzzy inference system (ANFIS) parameters via Box-Behnken experimental design approach: The prediction of chromium adsorption,” *Heliyon*, vol. 10, no. 3, Feb. 2024, doi: 10.1016/j.heliyon.2024.e25813.

[6] S. Sumarlinda, A. Binti Rahmat, Z. Binti, A. Long, and W. Lestari, “THE IMPROVEMENT PREDICTION MODEL USING ANFIS FOR MEDICAL DATASET,” *J Theor Appl Inf Technol*, vol. 15, no. 5, 2024.

[7] T. Eltaeib and A. Mahmood, “Differential evolution: A survey and analysis,” *Applied Sciences (Switzerland)*, vol. 8, no. 10, Oct. 2018, doi: 10.3390/app8101945.

[8] P. Tiwari, V. N. Mishra, and R. P. Parouha, “Optimization of numerical and engineering problems using altered differential evolution algorithm,” *Results in Control and Optimization*, vol. 14, Mar. 2024, doi: 10.1016/j.rico.2024.100377.

[9] S. Biswas *et al.*, “Integrating Differential Evolution into Gazelle Optimization for advanced global optimization and engineering applications,” *Comput Methods Appl Mech Eng*, vol. 434, Feb. 2025, doi: 10.1016/j.cma.2024.117588.

[10] J. Brest and M. Sepesy Maučec, “Comparative Study of Modern Differential Evolution Algorithms: Perspectives on Mechanisms and Performance,” *Mathematics*, vol. 13, no. 10, May 2025, doi: 10.3390/math13101556.

[11] P. Mishra, M. Ali, Pooja, and S. Islam, “Enhanced mutation strategy based differential evolution for global optimization problems,” *PeerJ Comput Sci*, vol. 11, 2025, doi: 10.7717/peerj-cs.2696.

[12] N. Guler, Z. Ben, A. Gunes, and F. Saidi, "Green Technologies and Sustainability Adaptive Neuro-Fuzzy Inference System-Genetic Algorithm approach for global maximum power point tracking in PV systems under different shading conditions," *Green Technologies and Sustainability*, vol. 3, no. 4, p. 100239, 2025, doi: 10.1016/j.grets.2025.100239.

[13] A. P. Kumar, Y. Macha, and A. S. Kumar, "HEART FAILURE DETECTION USING OPTIMIZATION ALGORITHMS," *J Theor Appl Inf Technol*, vol. 15, no. 7, 2025.

[14] P. J. Babu and A. Geetha, "EAI Endorsed Transactions Investigation on ANFIS-GA controller for speed control of a BLDC fed hybrid source electric vehicle," vol. 11, pp. 1–8, 2024, doi: 10.4108/ew.4965.

[15] H. E. Elzain *et al.*, "ANFIS-MOA models for the assessment of groundwater contamination vulnerability in a nitrate contaminated area," *J Environ Manage*, vol. 286, May 2021, doi: 10.1016/j.jenvman.2021.112162.

[16] M. Zanganeh, "Improvement of the ANFIS-based wave predictor models by the Particle Swarm Optimization," *Journal of Ocean Engineering and Science*, vol. 5, no. 1, pp. 84–99, 2020, doi: 10.1016/j.joes.2019.09.002.

[17] A. Pasha *et al.*, "Leveraging ANFIS with Adam and PSO optimizers for Parkinson's disease," *Heliyon*, vol. 10, no. 9, May 2024, doi: 10.1016/j.heliyon. 2024.e30241.

[18] I. M. El-Hasnony, S. I. Barakat, and R. R. Mostafa, "Optimized ANFIS Model Using Hybrid Metaheuristic Algorithms for Parkinson's Disease Prediction in IoT Environment," *IEEE Access*, vol. 8, pp. 119252–119270, 2020, doi: 10.1109/ACCESS.2020.3005614.

[19] S. Ghordoyee Milan, A. Roozbahani, N. Arya Azar, and S. Javadi, "Development of adaptive neuro fuzzy inference system –Evolutionary algorithms hybrid models (ANFIS-EA) for prediction of optimal groundwater exploitation," *J Hydrol (Amst)*, vol. 598, Jul. 2021, doi: 10.1016/j.jhydrol.2021.126258.

[20] N. Nguyen, "Designing a Novel Hybrid Fuzzy ~ GWO ~ PID Load-Frequency Controller for a complicated Large-Scale Four-Area interconnected Power Grid with RES and SMES," vol. 15, no. 3, pp. 23217–23223, 2025.

[21] D. Mazumdar, P. K. Biswas, C. Sain, F. Ahmad, and L. Al-fagih, "OPEN A robust MPPT framework based on GWO-ANFIS controller for grid- tied EV charging stations," pp. 1–21, 2024.

[22] R. Alkhanbouli, H. Matar, A. Almadhaani, F. Alhosani, M. Can, and E. Simsekler, "The role of explainable artificial intelligence in disease prediction : a systematic literature review and future research directions," *BMC Med Inform Decis Mak*, vol. 6, 2025, doi: 10.1186/s12911-025-02944-6.

[23] J. Devnath, F. Wahid, and A. Habib, "INTEROPERABILITY AND EXPLAINABILITY OF MACHINE LEARNING CLASSIFIERS TO DETECT LUNG CANCER," *J Theor Appl Inf Technol*, vol. 15, no. 21, 2023.

[24] F. Tuz, N. Hasan, and A. Rajbongshi, "An explainable AI-based approach for predicting undergraduate students' academic performance," *Array*, vol. 26, no. March, p. 100384, 2025, doi: 10.1016/j.array.2025.100384.

[25] V. Vimbi, N. Shaffi, and M. Mahmud, "Interpreting artificial intelligence models: a systematic review on the application of LIME and SHAP in Alzheimer's disease detection," Dec. 01, 2024, *Springer Science and Business Media Deutschland GmbH*. doi: 10.1186/s40708-024-00222-1.

[26] N. G. Rezk, S. Alshathri, A. Sayed, E. E. Hemdan, and H. El-behery, "XAI-Augmented Voting Ensemble Models for Heart Disease Prediction: A SHAP and LIME-Based Approach," 2024.

[27] A. Sathyan, A. I. Weinberg, and K. Cohen, "Interpretable AI for bio-medical applications," *Complex Engineering Systems*, vol. 2, no. 4, Dec. 2022, doi: 10.20517/ces.2022.41.

[28] S. Wang, H. Budiman, S. Ramadhani, T. FooNg, and F. Morsidi, "Review of Original Differential Evolution Algorithm: Research Trends, Original Setting Parameters," *Jurnal CoreIT: Jurnal Hasil Penelitian Ilmu Komputer dan Teknologi Informasi*, vol. 10, no. 2, p. 75, Nov. 2024, doi: 10.24014/coreit.v10i2.29903.

[29] S. Biswas *et al.*, "Integrating Differential Evolution into Gazelle Optimization for advanced global optimization and engineering applications," *Comput Methods Appl Mech Eng*, vol. 434, Feb. 2025, doi: 10.1016/j.cma.2024.117588.

[30] G. Visani, E. Bagli, and F. Chesani, "OptiLIME: Optimized LIME Explanations for Diagnostic Computer Algorithms," Jun. 2020, [Online]. Available: http://arxiv.org/abs/2006.05714

[31] V. Vimbi, N. Shaffi, and M. Mahmud, "Interpreting artificial intelligence models: a systematic review on the application of LIME and SHAP in Alzheimer's disease detection," Dec. 01, 2024, *Springer Science and Business Media Deutschland GmbH*. doi: 10.1186/s40708-024-00222-1.

[32] S. Dehdar Karsidani, M. Farhadian, H. Mahjub, and A. Mozayanimonfared, "Intelligent prediction of major adverse cardiovascular events (MACCE) following percutaneous coronary intervention using ANFIS-PSO model," *BMC Cardiovasc Disord*, vol. 22, no. 1, pp. 1–8, 2022, doi: 10.1186/s12872-022-02825-0.

[33] H. E. Elzain *et al.*, "ANFIS-MOA models for the assessment of groundwater contamination vulnerability in a nitrate contaminated area," *J Environ Manage*, vol. 286, May 2021, doi: 10.1016/j.jenvman.2021.112162.

[34] G. Gokkus, "ANFIS-based improved GWO: Rapid prototyping of low-power solar energy system under fast-changing solar radiation conditions," *J Radiat Res Appl Sci*, vol. 17, no. 2, p. 100920, Jun. 2024, doi: 10.1016/j.jrras.2024.100920.

[35] P. Tiwari, V. N. Mishra, and R. P. Parouha, "Optimization of numerical and engineering problems using altered differential evolution algorithm," *Results in Control and Optimization*, vol. 14, Mar. 2024, doi: 10.1016/j.rico.2024.100377.